

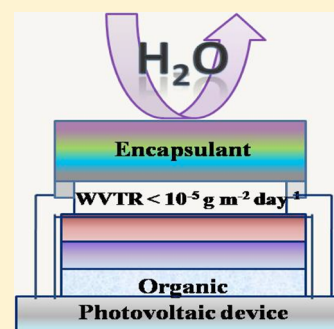
Layer-by-Layer Assembly of Nafion on Surlyn with Ultrahigh Water Vapor Barrier

Sindhu Seethamraju,[†] Arun D Rao,[‡] Praveen C Ramamurthy,^{†,‡} and Giridhar Madras^{*,†}

[†]Centre for Nanoscience and Engineering and [‡]Department of Materials Engineering, Indian Institute of Science, Bangalore, 560012, India

Supporting Information

ABSTRACT: A layer-by-layer approach was used for the fabrication of multilayer films for ultra high gas barrier applications. The ultra high gas barrier material was designed by incorporating Nafion layer in between bilayers of poly(ethylene imine) and poly(acrylic acid) on a Surlyn substrate. When the barrier film with self-assembled Nafion is exposed to the moist environment, Nafion absorbs and desorbs water molecules simultaneously, thereby reducing the ingress of moisture in to the film. In order to study the effect of Nafion, the fabricated barrier materials with and without the presence of Nafion were tested for water vapor barrier properties. The barrier films were further used for encapsulating organic photovoltaic devices and were evaluated for their potential use in barrier applications. The devices encapsulated with the films containing Nafion exhibited better performance when subjected to accelerated aging conditions. Therefore, this study demonstrates the effectiveness of self-assembled Nafion in reducing the water vapor permeability by nearly five orders of magnitude and in increasing the lifetimes of organic devices by ~ 22 times under accelerated weathering conditions.



1. INTRODUCTION

Flexible gas barrier materials are required for encapsulating organic devices such as light emitting diodes and organic photovoltaic (OPV) devices with ultralow water vapor transmission rates (WVTR) of $\sim 1 \times 10^{-6} \text{ g m}^{-2} \text{ day}^{-1}$ and oxygen transmission rates (OTR) of $\sim 1 \times 10^{-5} \text{ cc m}^{-2} \text{ day}^{-1} \text{ atm}^{-1}$.^{1–3} Various chemical and physical vapor deposition based techniques have been used for coating inorganic layers on to flexible substrates.^{4,5} However, high gas barriers are not achieved in these packaging materials because of pinhole-mediated permeation, absorption and adsorption of water/oxygen in these materials.^{6,7} Further, commercialization of encapsulating materials requires easy processability and economic feasibility for industrial scalability. Therefore, this work is aimed at the development of ultra low moisture permeable encapsulant with a functional layer, based on the layer-by-layer (LBL) technique.

In LBL deposition, the polymer layers assemble on the surface of substrate based on pH, concentration and temperature, when the substrate is sequentially immersed in polyelectrolyte solutions of opposite charges. The layers are held on to the substrate by electrostatic, hydrogen bond, and other weak/noncovalent interactions between the layers. LBL deposition of organic and inorganic nanoparticles has been used in designing various biomimetic and nanofunctional materials because of the possibility of creating controlled nanostructures for various applications.^{8,9} Few studies have investigated the development of oxygen barrier materials by employing LBL technique to assemble flakes of nanoclays and graphene oxide on to various substrates.^{10–12} Nano self-assemblies of poly(ethylene imine) (PEI) and poly(acrylic acid)

(PAA) have been previously studied for oxygen and moisture barrier properties.^{13,14}

Nafion is a perfluoro-sulfonated ionomer with hydrophobic fluorinated backbone and hydrophilic sulfonic acid groups. It is widely used in fuel cell and sensing applications because of its high proton conduction properties.^{15,16} Different water uptake characteristics from liquid and vapor phase are observed in Nafion resulting in Schroeder's paradox¹⁷ with water absorption being 2 orders of magnitude slower from vapor than from liquid.¹⁸ The transport of water in Nafion membranes is due to both diffusion and electro-osmotic drag.¹⁹ A single molecule of sulfonic acid group in Nafion is capable of associating with up to 23 molecules of H_2O .²⁰ The capillary porous sorption of water from liquid/vapor phase in Nafion is dependent on the level of hydration and thickness of the membrane.²¹ The absorbed water molecules form microsegregated clusters, which connect for small periods providing pathway for molecular transport.^{22,23} Desorption of water from hydrated Nafion occurs at a faster rate than absorption at the Nafion/gas interface. Therefore, Nafion was chosen because of the unique property of simultaneous capillary sorption and desorption. Nafion has been introduced in the barrier film to decrease water vapor permeability, in our work.

In our previous study,²⁴ Surlyn was used to fabricate blends because of its superior moisture barrier properties, solvent resistance and higher resilience compared to other commercially available polymers. Surlyn is an ionomer with pendant

Received: August 18, 2014

Revised: September 19, 2014

Published: November 12, 2014

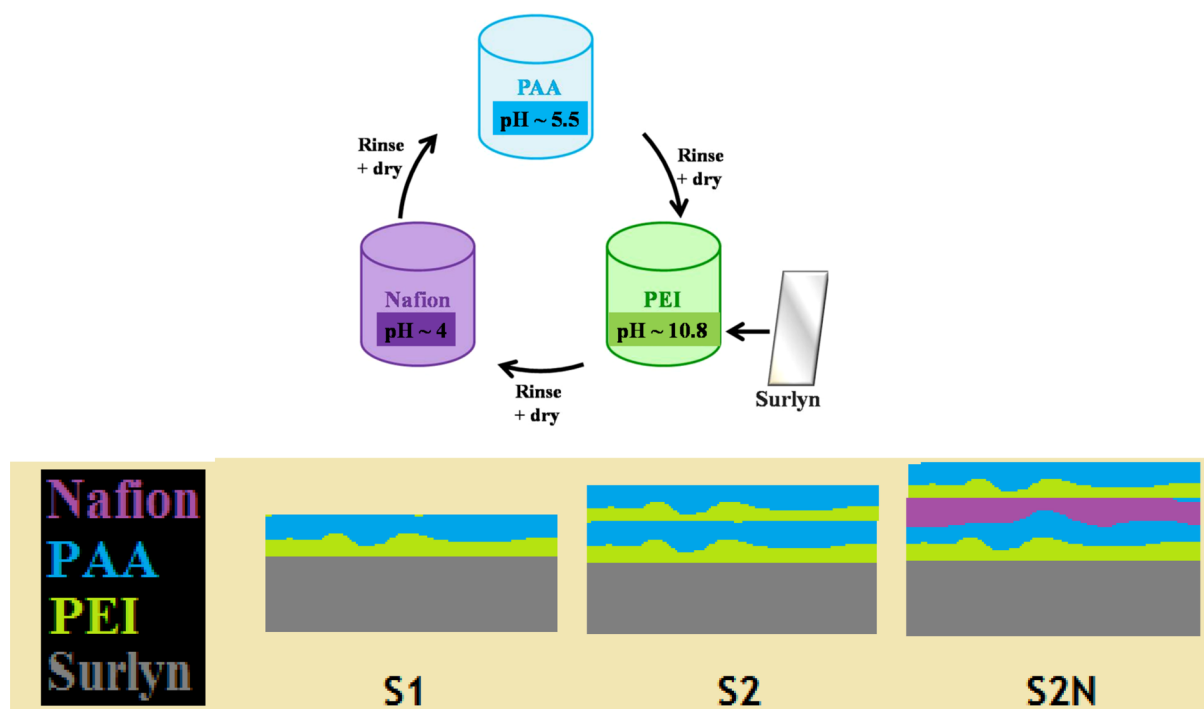


Figure 1. Schematic for self-assembling of PEI, PAA and Nafion layers for S1 (Surlyn/PEI/PAA), S2 (Surlyn/PEI/PAA/PEI/PAA), and S2N (Surlyn/PEI/PAA/Nafion/PEI/PAA) barrier films.

methacrylic acid groups and methylene backbone. Hence, Surlyn film was chosen as the substrate for providing support to the Nafion layer. Nafion is an anionic polyelectrolyte ionomer and has been previously used in LBL assembly for various other applications.^{25,26} The process of layer-by-layer is a well known technique that is robust, simple, and easily scalable for industrial applications. Poly(ethylene imine) (PEI) and poly(acrylic acid) have been used for the fabrication of self-assembled layers due to their cationic and anionic electrolytic nature. Branched PEI with $-\text{NH}_2$ groups at the ends was chosen so that it can interact electrostatically with PAA and Nafion during self-assembly. Nafion has been incorporated in the layered assemblies of poly(ethylene imine) (PEI) and poly(acrylic acid) (PAA) over Surlyn substrate. The fabricated functional barrier films were characterized for water vapor barrier properties and shown to be suitable for organic photovoltaic encapsulation applications.

2. EXPERIMENTAL SECTION

2.1. Chemicals. Surlyn (9 wt % methacrylic acid), branched poly(ethylene imine) ($M_w \approx 25\,000$), poly(acrylic acid) ($M_w \approx 400\,000$), Nafion perfluorinated resin solution (eq wt ≈ 1100), PCBM and PEDOT-PSS were purchased from Sigma-Aldrich Ltd (St. Louis, MO). Dichlorobenzene of $\sim 99.5\%$ purity was obtained from S.D. Fine Chem. (India) and was used without any further purification. Poly(3-hexylthiophene) (P3HT) was purchased from Rieke Metals Inc. (USA). The sealant used in calcium degradation and accelerated aging experiments, Lapox L12, was purchased from Atul Industries, Ltd. (India).

2.2. Material Fabrication. Surlyn pellets were melt compressed at 200 N cm^{-2} and $150\text{ }^\circ\text{C}$ to obtain films of thickness $\sim 50\text{ }\mu\text{m}$. These films were treated under UV light for 1 min prior to LBL deposition to provide active sites. The self-assembling of polycations and polyanions was achieved by dipping the treated Surlyn films into series of PEI ($\sim 1\text{ mg mL}^{-1}$, pH ~ 10.8), PAA (1 mg mL^{-1} , pH ~ 5.5) and Nafion (0.5 mg mL^{-1} , pH ~ 4) aqueous solutions consecutively for 1 min in each. After each immersion in polyelectrolyte, the film was thoroughly

washed with DI water to remove loosely bound layers and dried under nitrogen (Figure 1).

Three samples were fabricated in order to study the effect of Nafion on gas barrier properties. A bilayer consists of a layer of PEI and a layer of PAA. The first two samples include 1 (S1) and 2 (S2) bilayers of PEI and PAA. The third sample consists of Nafion in between two bilayers of PEI/PAA in S2 and was designated as S2N. Surlyn film (without any LBL deposition) is designated as S0.

2.3. Material Characterization. The LBL assembled films were gravimetrically characterized using Essae Teraoka microbalance with a sensitivity of 0.1 mg . FTIR characterization of all the layered films was carried out with Thermo-Nicolet (6700) IR spectrometer in the range 400 to 4000 cm^{-1} at 4 cm^{-1} interval. The thickness of the deposited layers was determined from Dektak surface profilometry. The UV-visible analysis absorption studies were carried out using PerkinElmer (Lambda-35) UV-visible spectrometer from 230 to 1100 nm interval. Contact angle measurements were conducted on Holmarc contact angle instrument (HO-IAD-CAM-O1A) dispensing $3\text{ }\mu\text{L}$ of DI water onto the barrier films from automatic dispenser with a microliter syringe.

2.4. WVTR Measurement with Cavity Ring Down Spectroscopy (CRDS)-Based Permeability Setup. A patented, CRDS-based water vapor permeability measurement setup²⁷ was used to measure WVTR through the fabricated barrier films. CRDS uses the principle of extinction of light in an enclosed cavity with highly reflecting monochromatic mirrors. When the analyte is present in cavity, the intensity of the light pulse decays at faster rate. On the basis of decay time, the concentration of the analyte can be determined up to ppt level. Therefore, Tiger optics CRDS (HALO+ 500) with moisture analyzer is used to determine WVTR up to $1 \times 10^{-6}\text{ g m}^{-2}\text{ day}^{-1}$. In this CRDS-based WVTR measurement setup, Extech temperature ($\pm 1\text{ }^\circ\text{C}$) and humidity ($\pm 3\%$ RH) sensors (RH520), Honeywell mass flow meter (AWM5200), and Kaleidoscope humidity chamber (KEW/PHC-80) were used. Stainless steel (316 L) and copper tubing (10 Ra surface finish) were used for the flow lines. These were connected using VCR fittings. Nitrogen leak rate was determined to be $< 2 \times 10^{-8}\text{ mbar L/s}$ for this setup.

This setup (Figure 2a) consists of a sample chamber where the barrier film is placed between two flanges (upper and lower). The

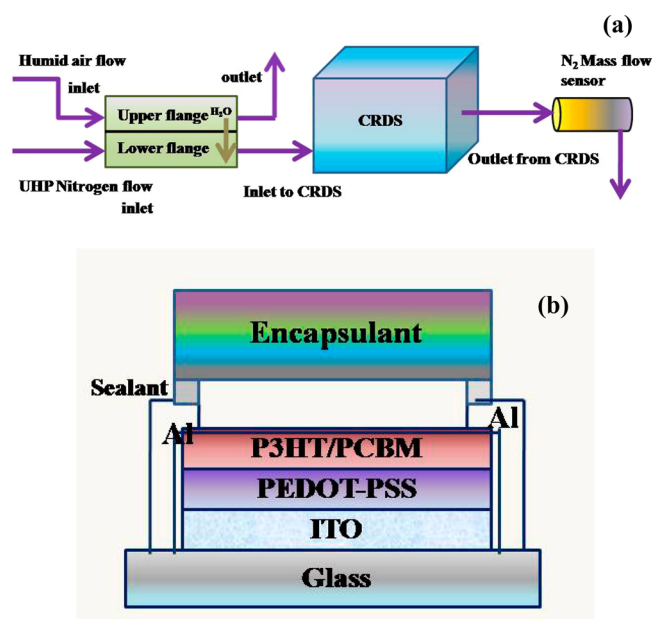


Figure 2. Schematic for (a) CRDS-based water vapor permeability measurement setup, (b) organic photovoltaic device.

upper flange is pumped with air of 93% RH from the humidity chamber, while the lower flange is purged with nitrogen. The moisture permeates through the film from the upper flange toward the lower flange. The lower flange is connected to the inlet of CRDS. The outlet from the CRDS is connected to a nitrogen mass flow meter.

Initial stabilization of CRDS was attained by purging nitrogen gas along both the lower and upper flanges. This also removes adsorbed moisture from the flow lines. After attaining steady state (C_0), the upper flow line was pumped with air of 93% RH. When the moisture permeates through the sample the concentration of the H_2O (analyte) increases in the enclosure of CRDS. This increase in concentration of H_2O (C_t) is continuously monitored by CRDS. The difference in C_t and C_0 gives the WVTR by following eq 1, where N_{flow} is the nitrogen flow rate and A is the effective area of the sample exposed to humid air.

$$WVTR = \frac{(C_t - C_0)(18N_{flow})}{(A \times 10^9)} \quad (1)$$

The results for WVTR from CRDS have been validated with the results from MOCON analyzer initially (see Figure S1a, b in the Supporting Information). Further, the WVTR through various polymers such as polyethylene, poly(vinyl alcohol), poly(methyl methacrylate), polypropylene, etc., have been determined in the prior work and compared with existing literature.²⁸

2.5. Aging Experiments. Organic photovoltaic (OPV) devices (Figure 2 (b)) based on P3HT/PCBM were fabricated and encapsulated with the barrier films inside glovebox. PEDOT-PSS was spin coated at 1000 rpm for 1 min on to ITO-coated glass slide and annealed to 110 °C. Fifteen mg of P3HT:PCBM (1:1) were dissolved in 1 mL of dichlorobenzene and was spin coated over PEDOT-PSS layer. All these slides were annealed at 125 °C for 15 min and aluminum electrodes were thermally evaporated (100 nm) at 2×10^{-6} mbar. The OPVs were sealed with barrier films using epoxy sealing at the edges. The devices were then placed in accelerated conditions of 85% RH and 65 °C for accelerated aging studies. Current voltage ($I-V$) characteristics and efficiencies of the non-encapsulated and encapsulated OPVs were measured using Keithley Semiconductor Characterization System (4200) and the solar simulator (sol 3 A, Newport Oriel), which is calibrated to 1 sun using standard Si diode (NREL) at various time intervals.

3. RESULTS AND DISCUSSION

Poly(ethylene-imine) (PEI) and poly(acrylic acid) (PAA) as cationic and anionic binders were deposited onto Surlyn films by self-assembly followed by Nafion layer. The schematic for LBL assembly of bilayers of PEI/PAA with and without Nafion layer is shown in Figure 1. The self-assembled layers of PEI/PAA/Nafion/PEI/PAA act as interacting moisture barrier between the environment and Surlyn substrate, resulting in ultra low permeabilities.

3.1. Film Properties. To verify the presence of polyelectrolyte layers on Surlyn, FTIR analysis was carried out and the IR spectrum for the fabricated barrier films is given in Figure 3. IR (Surlyn/PEI/PAA/Nafion): $\nu = 3527$ (s,

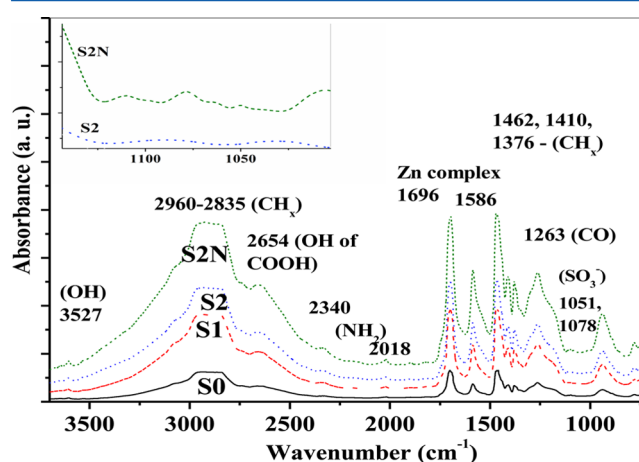


Figure 3. FTIR analysis for neat and all the LBL deposited Surlyn films (inset: characteristic peaks for suphonic acid groups in Nafion of S2N).

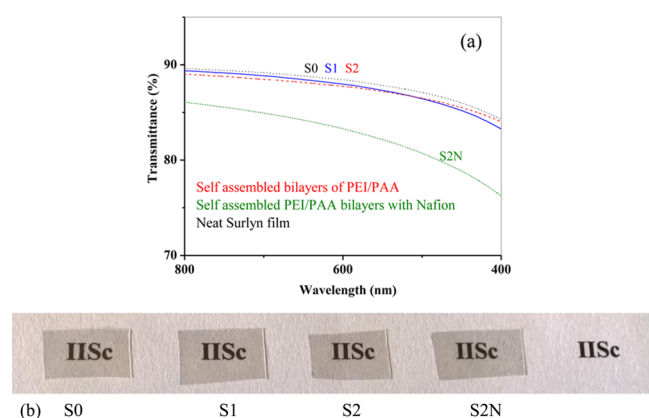
$\nu_s(\text{OH})$), 2835–2960 ($\nu_s(\text{C-H})$), 2654 ($\nu_s(\text{H-bonded OH of carboxylic acid})$), 1696, 1586 (ν_s , tetra coordinated zinc complexes), 1462, 1410, 1376 ($\nu_s(\text{CH}_2 \text{ \& \& CH}_3)$), 1263 ($\nu_s(\text{CO})$) cm^{-1} ; (Nafion): $\nu = 1051, 1078, 1096$ (w, $\nu_s(\text{SO}_3^-)$), 1472 (ν_s (w, (R-SO₃H)) cm^{-1} ; (PEI): $\nu = 3328, 2340$ ($\nu_s(\text{NH}_2)$), 2018 (w, $\nu_s(\text{NH}_2)$) cm^{-1} . The small peak at 3527 cm^{-1} correspond to the stretchings of hydroxyls of carboxylic acid groups in Surlyn and PAA. The broad band in the region 2835–2960 cm^{-1} is due to the presence of various C–H groups of Surlyn, PEI, and PAA. The broadened peak at 1263 cm^{-1} correspond to the stretching of CO groups. The above-discussed peaks are observed in all the films as the –OH, –COOH, and –CH_x groups are present in all cases. The stretching and bending vibrations for the amine groups at 2340 and 2018 cm^{-1} suggest the deposition of PEI in the films (S1, S2, and S2N). The minor peaks in the region 1050–1100 cm^{-1} for the film S2N (and absent in S0, S1, S2) indicate the presence of sulfonic acid groups of Nafion. The increase in weight of the neat Surlyn film after the deposition of PEI/PAA bilayers and Nafion layer was determined. The gravimetric change in the samples increased with the number of depositions (Table 1).

The thickness of deposition over Surlyn film was found to be 58, 116, and 145 nm (± 5 nm) for S1, S2, and S2N films, respectively. These values show that the Nafion layer has a thickness of ~ 30 nm. Visible light transparency of the barrier film is important for organic device encapsulation applications. Neat Surlyn (S0) was $\sim 89\%$ transparent in visible region (Figure 4a). The deposition of bilayers of PEI/PAA did not

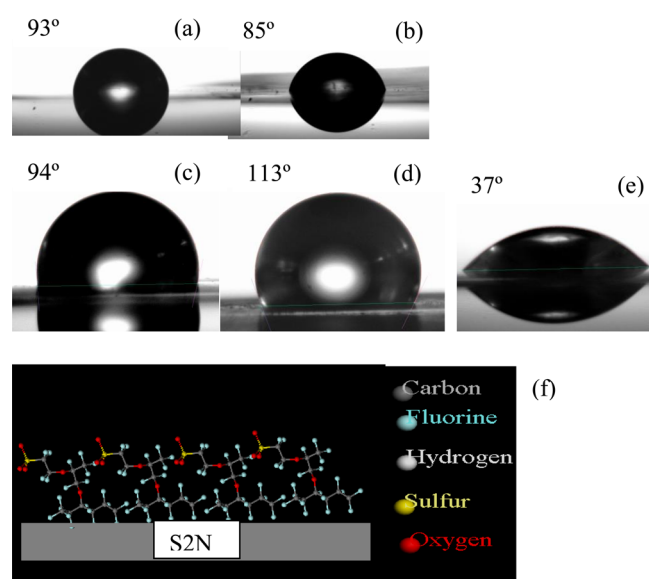
Table 1. Gravimetric Analysis for the LBL Assembly of PEI/PAA/Nafion over Surlyn Film

sample	no. of bilayers	no. of Nafion layers	total no. of layers	increase in weight (%)	visible-light transparency (%)	contact angle*
S0					89	86
S1	1		2	0.1	88	94
S2	2		4	0.2	88	113
S2N	2	1	5	0.3	85	37

*The measurements for contact angle include an error bar of $\pm 2^\circ$.

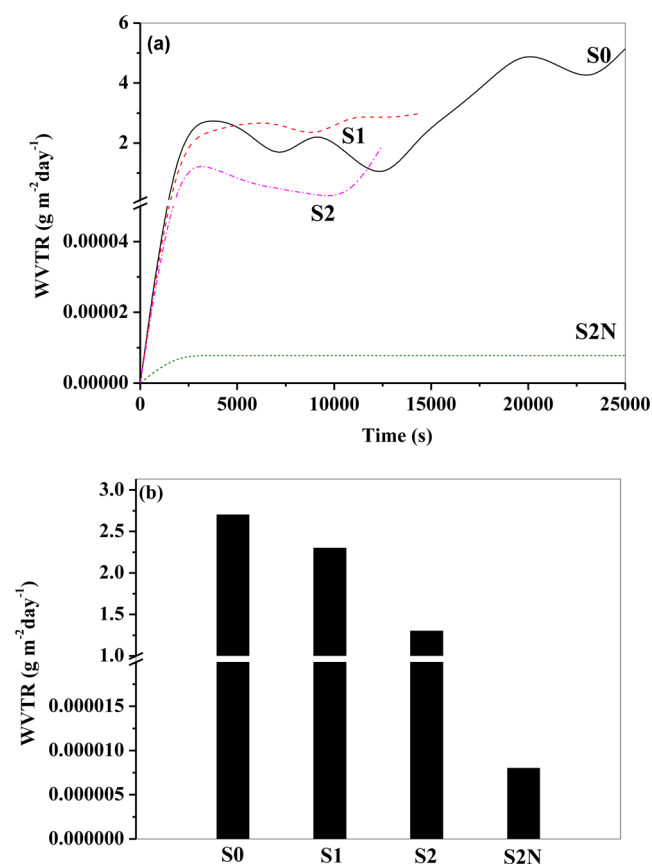
**Figure 4.** (a) UV-visible transparency and (b) image depicting the transparency of the barrier films.

significantly affect the transparency of neat Surlyn film (S0) and the films S1 and S2, retained transparencies up to 88%. For the barrier film with Nafion, S2N, the transparency decreased to $\sim 84\%$. However, the visual transparency of the Surlyn films was not affected after the deposition of PEI, Nafion and PAA layers of overall thickness ~ 145 nm (Figure 4b). Water contact angle measurements were carried out to determine the change in surface wettabilities with the assembling of various layers on Surlyn (Table 1 and Figures 5a–g). The knowledge of surface

**Figure 5.** Contact angle measurements for (a) neat-S0, (b) UV-treated S0, (c) S1, (d) S2, and (e) S2N; and (f) schematic for the arrangement of sulfonic acid groups of Nafion.

wetting helps in understanding if sulfonic acid groups are located closer to the interface of the surface/environment, which influences the moisture exchange properties. The contact angle for Surlyn film (S0) was $\sim 95^\circ$, which decreased to $\sim 84^\circ$ after UV treatment for 1 min. With the deposition of two bilayers (S2) of PEI/PAA, the contact angle increased to $\sim 113^\circ$. Though PEI/PAA is a hydrophilic system, the contact angle increased with increasing the number of PEI/PAA depositions. This could be due to the reduction in roughness of the samples. When a single Nafion layer (S2N) was introduced in between the two bilayers of PEI/PAA on Surlyn, the contact angle decreased to $\sim 37^\circ$, suggesting the increase in hydrophilicity because of the presence of SO_3^- groups. This suggests that the S2N film has SO_3^- groups on the surface, which can interact with moisture present in environment.

3.2. Water Vapor Barrier Properties. To verify the proposed mechanism of Nafion layer being able to exchange water vapor with the surroundings, the WVTR experiments for all the films were conducted using cavity ring down spectroscopy (CRDS) based setup (Figure 6). The WVTR

**Figure 6.** (a) Water vapor barrier measurements from CRDS-based setup, (b) WVTR profile for all the barrier samples.

for the neat Surlyn film (S0) was found to be $\sim 2.7 \text{ g m}^{-2} \text{day}^{-1}$. With the deposition of bilayer/s of PEI/PAA on to Surlyn, for S1 and S2, the measured WVTRs were 2.3 and 1.3 $\text{g m}^{-2} \text{day}^{-1}$ after 10 000 s, respectively. This shows that the water vapor permeability decreased by 14% and 52% from S0 to S1 and S2, respectively. However, only a reduction of 44% and 22% in WVTR was observed when the number of bilayers of PEI/PAA were increased to 4 and 8, respectively (see Figure S2a in the Supporting Information). When a single Nafion layer was used

in the LBL assembly, the WVTR was found to be as low as $\sim 8 \times 10^{-6} \text{ g m}^{-2} \text{ day}^{-1}$ for more than 12 h exposure to humid air flow. When the film S2N was exposed to humid environment, Nafion will absorb and desorb moisture simultaneously. Therefore, moisture will not permeate in to the Surlyn film below the Nafion layer. This resulted in the reduction of WVTR for S2N film by five orders when compared to the neat Surlyn (S0) and PEI/PAA-coated Surlyn films (S1, S2). However, increasing the number of Nafion layers did not result in better moisture barrier (see Figure S2b in the Supporting Information). This could be due to the presence of SO_3^- groups away from the surface which can be confirmed from the increasing contact angle with increasing number of Nafion layers (see Figure S3 in the Supporting Information). Therefore, S2N film is more effective as water vapor barrier when compared to the other fabricated barrier films with the demonstrated moisture exchange mechanism for its applicability in high barrier materials.

3.3. OPV Accelerated Aging Studies. To evaluate the suitability of the fabricated material as an encapsulant, OPV devices were encapsulated and subjected to accelerated aging conditions (65°C and 85% RH). The lifetimes of the devices under these accelerated conditions are equivalent to ~ 250 times the lifetimes at 25°C and 35% RH.²⁹ The device characteristics for each OPV device were determined before and after accelerated aging. The efficiencies were averaged for at least 4 devices and then normalized with aging time for every encapsulated device. The drop in the normalized efficiency with time for the encapsulated device is used to evaluate the performance of the encapsulant (Figure 7, eq 2).

$$\text{performance of the OPV (\%)} = 100 \frac{\eta_o - \eta_t}{\eta_o} \quad (2)$$

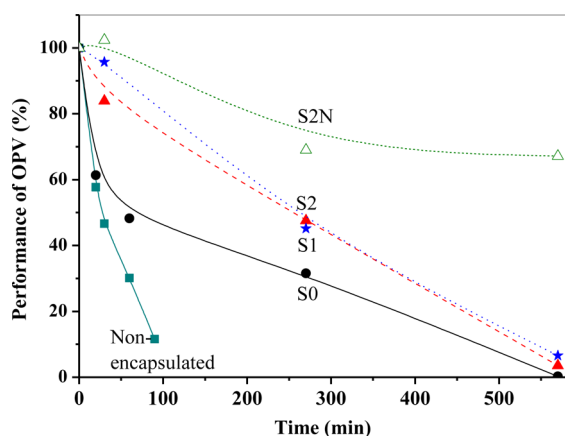


Figure 7. Device lifetime studies under accelerated aging conditions (65°C , 85% RH) for encapsulated OPVs.

In eq 2, η_o and η_t represent the normalized efficiencies for photovoltaic devices before aging at $t = 0$ and after aging for time t . After 30 min of accelerated aging, the performance of the non encapsulated device dropped to 45% of its initial value while it dropped to 55% for the device encapsulated with S0. This indicates that encapsulation with S0 is not very effective. However, the OPV devices encapsulated with S1 and S2 sustained $\sim 85\%$ of their initial activities. The devices with Nafion encapsulant (S2N) maintained $>95\%$ of their initial performances. The non encapsulated device completely lost its

current density in 90 min. Further aging the devices up to 270 min, the performances dropped to ~ 30 , 45, and 48% of their initial performances for S0, S1, and S2 encapsulated OPVs. The devices with S2N encapsulants showed $\sim 70\%$ of their initial performances after 270 min. After 570 min of accelerated aging, all the encapsulated OPVs (except for S2N encapsulant) lost their total performances. The OPV devices encapsulated with S2N films retained $\sim 70\%$ even after 570 min of accelerated aging. Therefore, it can be concluded that the S2N film is effective in reducing the water vapor permeation by decreasing the number of H_2O molecules reaching the OPV device. Such LBL assemblies with single Nafion layer can be used in coatings for various flexible packaging applications with low water vapor transmission requirements.

4. CONCLUSIONS

We have successfully designed a barrier material with ultra low water vapor permeability using self-assembled Nafion layer on Surlyn using PEI and PAA. The resulting barrier material with single Nafion layer in between two bilayers of PEI/PAA, exhibited WVTR $< 1 \times 10^{-5} \text{ g m}^{-2} \text{ day}^{-1}$. This suggests that Nafion layer was functional in reducing moisture ingress in to Surlyn when sulfonic acid groups are near the surface, in contact with the environment for exchanging moisture as observed for S2N film. For analyzing the exact nature and effect of Nafion in the LBL assembly with PEI and PAA, Surlyn films with self-assembled bilayers of PEI/PAA were also characterized for material and barrier properties. Because of the hygroscopic nature of PEI and PAA, the presence of bilayers of PEI/PAA did not significantly change the moisture barrier property of Surlyn. However, the addition of Nafion layer drastically reduced the WVTR by >5 orders.

The accelerated aging studies of OPVs for 570 min show that the OPVs encapsulated with S2N films were stable sustaining with at least 70% of their initial performances constantly. While for the other (S0, S1, and S2) encapsulated devices, the performances dropped down completely to $<5\%$. This shows that the barrier film with single Nafion layer is effective in functioning as an exchange medium for moisture absorption and desorption with the surroundings, resulting in an increase of the lifetimes of the OPV devices. Therefore, these studies demonstrate that ultra low WVTR can be achieved by the process of assembling single Nafion layer on to various substrates/surfaces for various barrier coating applications. Moreover, these self-assembled layers involve simple processing techniques suitable for large scale industrial processing of flexible organic electronic devices.

■ ASSOCIATED CONTENT

Supporting Information

Comparison for WVTR results from CRDS and MOCON based instruments for a test sample, water vapor barrier measurements for the barrier samples with four and eight bilayers of PEI/PAA depositions and two and three PEI/PAA/Nafion trilayers over Surlyn and the variation of contact angle with increasing the number of Nafion layers. This material is available free of charge via the Internet at <http://pubs.acs.org/>.

■ AUTHOR INFORMATION

Corresponding Author

*E-mail: giridhar@chemeng.iisc.ernet.in. Phone: 91-80-22932321.

Notes

The authors declare no competing financial interest.

■ ACKNOWLEDGMENTS

This work was supported by Science and Engineering Research Board, Department of Science and Technology (1362/2014).

■ REFERENCES

- (1) Norrman, K.; Larsen, N. B.; Krebs, F. C. Stability/degradation of polymer solar cells. *Sol. Energy Mater. Sol. Cells* **2006**, *90*, 2793–2828.
- (2) Reese, M. O.; Nardes, A. M.; Rupert, B. L.; Larsen, R. E.; Olson, D. C.; Lloyd, M. T.; Kopidakis, N. Photoinduced Degradation of Polymer and Polymer–Fullerene Active Layers: Experiment and Theory. *Adv. Funct. Mater.* **2010**, *20*, 3476–3483.
- (3) Norrman, K.; Gevorgyan, S. A.; Krebs, F. C. Water-Induced Degradation of Polymer Solar Cells Studied by H₂¹⁸O Labeling. *ACS Appl. Mater. Interface* **2008**, *1*, 102–112.
- (4) Dameron, A. A.; Davidson, S. D.; Burton, B. B.; Carcia, P. F.; McLean, R. S.; George, S. M. Gas Diffusion Barriers on Polymers Using Multilayers Fabricated by Al₂O₃ and Rapid SiO₂ Atomic Layer Deposition. *J. Phys. Chem. C* **2008**, *112*, 4573–4580.
- (5) Chou, C. T.; Yu, P. W.; Tseng, M. H.; Hsu, C. C.; Shyue, J. J.; Wang, C. C.; Tsai, F. Y. Transparent Conductive Gas-Permeation Barriers on Plastics by Atomic Layer Deposition. *Adv. Mater.* **2013**, *25*, 1750–1754.
- (6) Hanika, M.; Langowski, H. C.; Moosheimer, U.; Peukert, W. Inorganic Layers on Polymeric Films – Influence of Defects and Morphology on Barrier Properties. *Chem. Eng. Technol.* **2003**, *26*, 605–614.
- (7) Erlat, A. G.; Henry, B. M.; Grovenor, C. R. M.; Briggs, A. G. D.; Chater, R. J.; Tsukahara, Y. Mechanism of Water Vapor Transport through PET/AlO_xN_y Gas Barrier Films. *J. Phys. Chem. B* **2004**, *108*, 883–890.
- (8) *Multilayer Thin Films*; Decher, G., Schlenoff, J. B., Eds.; Wiley–VCH, Weinheim, Germany, 2003.
- (9) Matsusaki, M.; Ajiro, H.; Kida, T.; Serizawa, T.; Akashi, M. Layer-by-Layer Assembly Through Weak Interactions and Their Biomedical Applications. *Adv. Mater.* **2012**, *24*, 454–474.
- (10) Tzeng, P.; Maupin, C. R.; Grunlan, J. C. Influence of polymer interdiffusion and clay concentration on gas barrier of polyelectrolyte/clay nanobrick wall quadlayer assemblies. *J. Membr. Sci.* **2014**, *452*, 46–53.
- (11) Stevens, B. E.; Odenborg, P. K.; Priolo, M. A.; Grunlan, J. C. Hydrophobically Modified Polyelectrolyte for Improved Oxygen Barrier in Nanobrick Wall Multilayer Thin Films. *J. Polym. Sci. B: Polym. Phys.* **2014**, *52*, 1153.
- (12) Yang, Y.-H.; Bolling, L.; Priolo, M. A.; Grunlan, J. C. Super Gas Barrier and Selectivity of Graphene Oxide-Polymer Multilayer Thin Films. *Adv. Mater.* **2013**, *25*, 503.
- (13) Yang, Y. H.; Haile, M.; Park, Y. T.; Malek, F. A.; Grunlan, J. C. Super Gas Barrier of All-Polymer Multilayer Thin Films. *Macromolecules* **2011**, *44* (6), 1450–59.
- (14) Yang, Y. H.; Bolling, L.; Haile, M.; Grunlan, J. C. Improving oxygen barrier and reducing moisture sensitivity of weak polyelectrolyte multilayer thin films with crosslinking. *RSC Adv.* **2012**, *2*, 12355–63.
- (15) Divisek, J.; Eikerling, M.; Mazin, V.; Schmitz, H.; Stimming, U.; Volkovich, Y. M. A Study of Capillary Porous Structure and Sorption Properties of Nafion Proton-Exchange Membranes Swollen in Water. *J. Electrochem. Soc.* **1998**, *145*, 2677–2683.
- (16) Zhu, M.; Li, N.; Ye. Sensitive and Selective Sensing of Hydrogen Peroxide with Iron-Tetrakisulfophthalocyanine-Graphene-Nafion Modified Screen-Printed Electrode. *J. Electroanalysis* **2012**, *24*, 1212–1219.
- (17) Schroeder, P. Z. Über Erstarrungs-und Quellungserscheinungen von Gelatine. *Phys. Chem.* **1903**, *45*, 75.
- (18) Zhao, Q.; Majsztrik, P.; Benziger, J. Diffusion and Interfacial Transport of Water in Nafion. *J. Phys. Chem. B* **2011**, *115*, 2717–2727.
- (19) Fuller, T. F.; Newman, J. Experimental Determination of the Transport Number of Water in Nafion 117 Membrane. *J. Electrochem. Soc.* **1992**, *139*, 1332–1337.
- (20) Onishi, L. M.; Prausnitz, J. M.; Newman, J. Water–Nafion Equilibria. Absence of Schroeder's Paradox. *J. Phys. Chem. B* **2007**, *111*, 10166–10173.
- (21) Hietala, S.; Maunu, S. L.; Sundholm, F. Sorption and diffusion of methanol and water in PVDF-g-PSSA and Nafion® 117 polymer electrolyte membranes. *J. Polym. Sci.: B: Polym. Phys.* **2000**, *38*, 3277–3284.
- (22) Mauritz, K. A.; Moore, R. B. State of Understanding of Nafion. *Chem. Rev.* **2004**, *104*, 4535–4586.
- (23) Galperin, D. Y.; Khokhlov, A. R. Mesoscopic Morphology of Proton-Conducting Polyelectrolyte Membranes of Nafion® Type: A Self-Consistent Mean Field Simulation. *Macromol. Theory Simul.* **2006**, *15*, 137–146.
- (24) Seethamraju, S.; Ramamurthy, P. C.; Madras, G. Ionomer Based Blend as Water Vapor Barrier Material for Organic Device Encapsulation. *ACS Appl. Mater. Interfaces* **2013**, *5*, 4409–4416.
- (25) Kim, D. W.; Choi, H. S.; Lee, C.; Blumstein, A.; Kang, Y. Investigation on methanol permeability of Nafion modified by self-assembled clay-nanocomposite multilayers. *Electrochim. Acta* **2004**, *50*, 659–662.
- (26) Jiang, S. P.; Liu, Z.; Tian, Z. Q. Layer-by-Layer Self-Assembly of Composite Polyelectrolyte–Nafion Membranes for Direct Methanol Fuel Cells. *Adv. Mater.* **2006**, *18*, 1068–1072.
- (27) Ramamurthy, P. C.; Gupta, S.; Madras, G. Development of “Ultra Low Moisture Permeability Measurement Technique” using Cavity Ring Down Spectroscopy. IPEC 137/2012 1651/CHE/2012.
- (28) Seethamraju, S.; Ramamurthy, P. C.; Madras, G. Water Vapor Permeabilities through Polymers: Diffusivities from Experiments and Simulations. *Mater. Res. Express* **2014**, *1*, 035301.
- (29) Reese, M. O.; et al. Consensus stability testing protocols for organic photovoltaic materials and devices. *Sol. Energy Mater. Sol. Cells* **2011**, *95*, 1253–1267.